

experimental evidence. This calculation yields a positive  $s$ -band polarization; a full discussion is given in Ref. 6.

- <sup>18</sup>E. Clementi, IBM J. Res. Develop. **9**, 2 (1965).
- <sup>19</sup>T. Gilbert (private communication).
- <sup>20</sup>David Pines, *The Many Body Problem* (Benjamin, New York, 1952).
- <sup>21</sup>R. R. Sharma, J. Math. Phys. **9**, 505 (1968); K. J. Duff, Intern. J. Quantum Chem. (to be published).
- <sup>22</sup>P. O. Löwdin, Advan. Phys. **5**, 1 (1956).
- <sup>23</sup>M. E. Rose, *Elementary Theory of Angular Momentum* (Wiley, New York, 1957).
- <sup>24</sup>J. C. Phillips and L. Kleinman, Phys. Rev. **128**, 2098 (1963).
- <sup>25</sup>J. C. Phillips, Phys. Rev. **123**, 420 (1961).
- <sup>26</sup>William Brinkman and Bernard Goodman, Phys. Rev. **149**, 597 (1966).
- <sup>27</sup>G. D. Gaspari, Ph.D. dissertation, University of California, Riverside, 1964 (unpublished).

- <sup>28</sup>S. D. Mahanti, Ph.D. dissertation, University of California, Riverside, 1968 (unpublished).
- <sup>29</sup>J. Kanamori, Progr. Theoret. Phys. (Kyoto) **30**, 275 (1963).
- <sup>30</sup>M. C. Gutzwiller, Phys. Rev. **134**, A923 (1964).
- <sup>31</sup>A review of the experimental evidence supporting this is given by C. Herring, in *Magnetism*, edited by G. T. Rado and H. Suhl (Academic, New York, 1966), Vol. IV.
- <sup>32</sup>A. J. Blodgett and W. E. Spicer, Phys. Rev. **158**, 514 (1967).
- <sup>33</sup>D. E. Eastman, J. Appl. Phys. **40**, 1387 (1969).
- <sup>34</sup>D. H. Tomboulion and D. E. Bedo, Phys. Rev. **121**, 146 (1961).
- <sup>35</sup>M. Horowitz and J. G. Daunt, Phys. Rev. **91**, 1099 (1953).
- <sup>36</sup>A. V. Gold, J. Appl. Phys. **39**, 768 (1968).
- <sup>37</sup>R. C. Fivaz, J. Appl. Phys. **39**, 1278 (1968).
- <sup>38</sup>P. N. Dheer, Phys. Rev. **156**, 637 (1967).

PHYSICAL REVIEW B

VOLUME 3, NUMBER 1

1 JANUARY 1971

## Exciton-Exciton Transitions in $\text{MnF}_2$

S. E. Stokowski and D. D. Sell

*Bell Telephone Laboratories, Murray Hill, New Jersey 07974*

(Received 27 August 1970)

Transitions involving the simultaneous creation of two excitons in  $\text{MnF}_2$  are reported. These double excitons are combinations of the  $E1$  ( $18419.6 \text{ cm}^{-1}$ ) and  $E2$  ( $18436.6 \text{ cm}^{-1}$ ) single excitons. Line transition identified as  $E2 + E2$  ( $36789 \text{ cm}^{-1}$ ) and  $E1 + E2$  ( $36917 \text{ cm}^{-1}$ ) were seen; however, the transition to the  $E1 + E1$  state was not observed. The identification was made with the aid of uniaxial stress measurements; the energy shifts of the double excitons under stress are simply related to those of the  $E1$  and  $E2$  excitons. It is shown on the basis of one-electron molecular orbitals that for the  $E1 + E1$  state the exchange interaction, and thus the transition probability, is small. The observed polarization of the double exciton lines is explained in terms of the Mn pair symmetry. It has also been confirmed that the  $E1$  exciton transforms as the  $B_3$  representation of the group  $D_{2h}$ .

### I. INTRODUCTION

The study of antiferromagnetic insulators in recent years has led to the observation of double excitations, such as magnon-magnon,<sup>1,2</sup> exciton-magnon,<sup>3,4</sup> and exciton-exciton<sup>5,6</sup> transitions. These two-center excitations provide information about the magnon dispersion and density of states, molecular fields, and the exchange interaction between magnetic ions. In this paper we present and discuss the observation of double-exciton transitions in  $\text{MnF}_2$ . These transitions are the result of the absorption of a photon and the creation of two excitons in the lowest-energy  $^4T_1$  state of the  $\text{Mn}^{2+}$  ion.

Exciton and exciton-magnon absorption were first seen in  $\text{MnF}_2$  by Greene *et al.*<sup>3</sup> They observed exciton transitions, which they labeled  $E1$  ( $18419.6 \text{ cm}^{-1}$ ) and  $E2$  ( $18436.6 \text{ cm}^{-1}$ ), between the  $^6A_1$  ground state and two states of the  $^4T_1$  manifold of  $\text{Mn}^{2+}$ . Dietz, Missetich, and

Guggenheim<sup>7</sup> found, through uniaxial pressure experiments, that  $E1$  and  $E2$  could be characterized by linear combinations of the  $(\pm 1, \frac{3}{2})$  components of the  $^4T_1$  state. Because these two states are only  $17 \text{ cm}^{-1}$  apart, the effective spin-orbit parameter for the  $^4T_1$  state must be small. Some calculations have been done on the energy splittings of the  $^4T_1$  states, but with only limited success in explaining the experimentally observed splittings. Both Meltzer and Lohr<sup>8</sup> and Washimiya and Gondaira<sup>9</sup> suggested that the smallness of the spin-orbit coupling is due to vibronic interaction. Exciton-magnon fluorescence has been studied by Dietz and Missetich.<sup>10</sup> Their results indicate that the  $E1$  and  $E2$  excitons have no measurable dispersion, although later Dietz *et al.*<sup>11</sup> found a thermodynamic distinction between the zone-center and zone-boundary exciton states. Thus, for most purposes, the excitation can be considered as being localized on a particular ion.

Previously, exciton-exciton transitions were

seen by Ferguson<sup>5</sup> and by Van der Ziel and Guggenheim.<sup>6</sup> Ferguson made observations on the broad absorption bands in  $\text{MnF}_2$ ,  $\text{RbMnF}_3$ , and  $\text{KMnF}_3$ , and on the basis of their energies and temperature shifts, assigned some of the bands to phonon-assisted double-exciton transitions. In particular, for  $\text{MnF}_2$  at room temperature, he observed the  ${}^4T_1 + {}^4T_1$  band peak at  $38\,800\text{ cm}^{-1}$ , exactly at twice the energy of the single-exciton band peak at  $19\,400\text{ cm}^{-1}$ . We were able to see the pure electronic transitions which are the origin of this double-exciton band, and our results confirm his assignment. Van der Ziel and Guggenheim observed pure exciton-exciton transitions in  $\text{CoF}_2$  in which optical and low-energy excitons were created simultaneously.

We have observed pure electronic transitions in the region of  $36\,800\text{ cm}^{-1}$  and have identified the  $E2 + E2$  ( $36\,789\text{ cm}^{-1}$ ) and  $E1 + E2$  ( $36\,917\text{ cm}^{-1}$ ) transitions. The assignments were made on the basis of uniaxial stress experiments by relating the energy shifts of the lines to those of the single excitons, measured by Dietz *et al.*<sup>7</sup> This is described in detail in Sec. III. Interestingly, the transition  $E1 + E1$  was not seen, but this is explained in Sec. IV by demonstrating that there is little overlap between the one-electron orbitals involved in the transition for the two second-nearest-neighbor  $\text{Mn}^{2+}$  ions. In Sec. IV we also discuss the polarization of the double-exciton lines. It is shown there that the polarization of the transitions is restricted by the pair symmetry. It has also been confirmed on the basis of this work that the single exciton  $E1$  transforms as the  $B_3$  representation of the unitary  $D_{2h}$  site group; and  $E2$  as  $B_2$ . (The notation used here can be found in Tinkham's<sup>12</sup> book.)

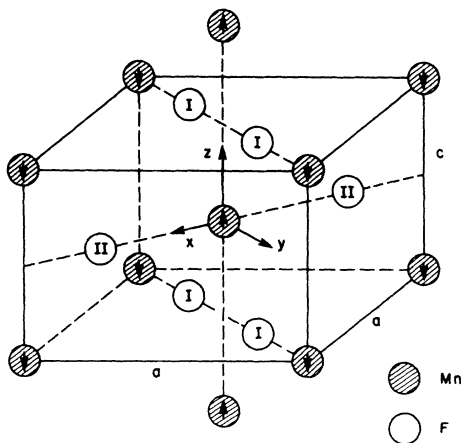


FIG. 1. Unit cell of  $\text{MnF}_2$ . The two types of fluorine neighbors of the body-center Mn ion are labeled by the Roman numerals.

The  $\text{MnF}_2$  unit cell is shown in Fig. 1. There are two sublattices with opposite spin on each. The center Mn ions on one sublattice are second nearest neighbors to the corner ions on the other sublattice. Each Mn ion has two types of fluorine neighbors: One, designated type II, lies along a  $\langle 110 \rangle$  direction and the other, designated type I, lies in a  $\{110\}$  plane. (This labeling of the Mn-F bond is identical to that of Tanabe and Gonda.<sup>13</sup> Meltzer and Lohr<sup>8</sup> used the opposite notation in their paper.) The coordinate system shown is a local system for each sublattice. Its orientation is defined by placing  $z$  parallel to the  $c$  axis and  $x$  along the direction to the type-II fluorines. The two sublattices are related by a  $90^\circ$  rotation about the  $c$  axis plus a spin flip.

## II. EXPERIMENTAL DETAILS

The absorption measurements were made with a double-beam spectrophotometer described in a previous paper.<sup>14</sup> Our detection system was shot-noise limited, the peak-to-peak shot-noise limit being four parts in  $10^3$  at  $2725\text{ \AA}$  with a resolution of  $0.2\text{ \AA}$ . The stress apparatus is similar to the apparatus used previously for modulated piezo-reflectance measurements.<sup>15</sup> Here we use the same pneumatic piston approach to apply dc stress to a sample mounted between copper end pads (no Epoxy used) and immersed in pumped liquid helium. The samples used in the pressure experiments were either  $1 \times 4 \times 5\text{ mm}$  or  $1 \times 5 \times 5\text{ mm}$ . Samples were from two sources, a boule of rather pure  $\text{MnF}_2$  grown by Guggenheim of Bell Telephone Laboratories and generously given to us by Dietz and a boule with  $0.1\%$  Ca impurity grown by Feigelson of Stanford University which was loaned to us by Holzrichter. There was no difference between the two samples as far as our results showed, except that the linewidths were slightly larger in the Ca-doped samples.

## III. RESULTS

The  $\vec{k}=0$  double-exciton states are combinations of two single excitons with opposite  $\vec{k}$  vectors. Thus, excitons over the complete Brillouin zone contribute to the double-exciton absorption. However, because the  $E1$  and  $E2$  exciton dispersion is small, we can make the assumption that the energy and basis states of  $E1$  and  $E2$  are the same throughout the zone. Therefore, if the exciton-exciton interaction effects are  $k$  independent, the energy of the  $k=0$  double exciton is independent of the  $k$  value of the single excitons. Thus, it is possible to describe the double-exciton transitions as transitions of pairs of ions.

In a transition the two excitons are created on different sublattices because, in this way, the total spin does not change. The creation of two excitons

on the same sublattice is a much weaker process since the total spin changes by two in this case. There are four possible combinations of the  $E1$  and  $E2$  excitons with one exciton on each sublattice of  $\text{MnF}_2$ . The possible double-exciton states are  $E1(A) + E1(B)$ ,  $E2(A) + E2(B)$ ,  $E1(A) + E2(B)$ , and  $E2(A) + E1(B)$ , where  $A$  and  $B$  refer to the two different sublattices. We shall refer to these transitions as  $E_{11}$ ,  $E_{22}$ ,  $E_{12}$ , and  $E_{21}$ , respectively.

The absorption spectrum at an energy just below the double-exciton band ( ${}^4T_1 + {}^4T_1$ ) identified by Ferguson is shown in Fig. 2. At 2K, the  $E_{22}$ ,  $E_{12}$ , and  $E'_{22}$  lines have the properties listed in Table I. Assignment of these lines was made on the basis of their response to uniaxial stress. The energy shift of a double-exciton transition due to stress is a sum of the shifts of the constituent single excitons plus any change in the exciton-exciton interaction energy. Our data are consistent with the assumption that there is no stress dependence of the exciton-exciton interaction; thus, identification of  $E_{22}$ ,  $E_{12}$ , and  $E'_{22}$  can be made simply from the known uniaxial stress shifts of the  $E1$  and  $E2$  excitons. Our stress results are shown in Fig. 3, where the solid lines show the energy shifts expected on the basis of the results of Dietz *et al.*<sup>7</sup> if no anticrossings occur. We mention the possibility of anticrossings because the single excitons  $E1$  and  $E2$  on one of the sublattices have an anticrossing at about  $10^3$  kg/cm<sup>2</sup> of  $[110]$  stress. However, no anticrossing of the double excitons is seen because the exciton-exciton interaction has separated the  $(E_{12}, E_{21})$  and  $E_{22}$  states by  $128$  cm<sup>-1</sup>.

Therefore, the anticrossing of these excitons is shifted beyond the region of reasonable pressures. An anticrossing between  $E_{11}$  and  $(E_{12}, E_{21})$  might have determined the unknown energy of  $E_{11}$ ; however, no evidence of any anticrossing was seen.

The stress behavior of  $E'_{22}$  is the same as  $E_{22}$ .

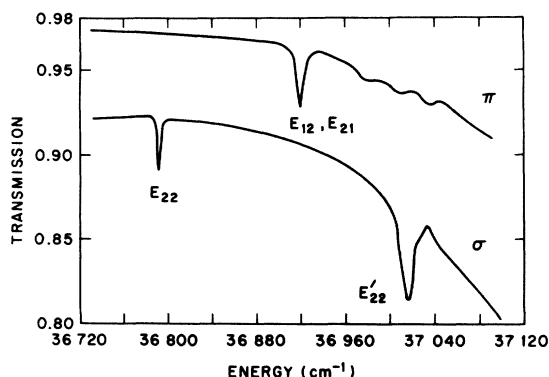


FIG. 2. Polarized transmission spectra of  $\text{MnF}_2$  at 2 K. The  $\alpha$  spectrum is identical to that in  $\sigma$  polarization. Sample length is 14 mm.

TABLE I. Properties of double-exciton lines at 2 K.

	Energy (cm <sup>-1</sup> )	Linewidth (cm <sup>-1</sup> )	Peak absorption coefficient (cm <sup>-1</sup> )	Oscillator strength	Polariz- ation
$E_{22}$	36 789	2	$2.2 \times 10^{-2}$	$2.8 \times 10^{-12}$	$\sigma, \alpha$
$E_{12}$	36 917	8.5	$2.3 \times 10^{-2}$	$1.2 \times 10^{-11}$	$\pi$
$E'_{22}$	37 012	14.5	$3.1 \times 10^{-2}$	$2.8 \times 10^{-11}$	$\sigma, \alpha$

Consequently, we identify  $E'_{22}$  as a transition involving an  $E_{22}$  double exciton plus one or more phonon or magnon excitations to account for the extra  $223$  cm<sup>-1</sup> of energy. The  $E'_{22}$  transition will not be considered further in this paper, although it is deserving of some additional study.

The energy of  $E_{22}$  lies  $84$  cm<sup>-1</sup> below that of twice the energy of  $E2$ , and  $(E_{12}, E_{21})$  lies  $61$  cm<sup>-1</sup> above the sum of the energies of  $E1$  and  $E2$ . This energy shift indicates a sizable exciton-exciton interaction. In contrast, the exciton-magnon interaction energy is only a few cm<sup>-1</sup>.<sup>10</sup> This difference

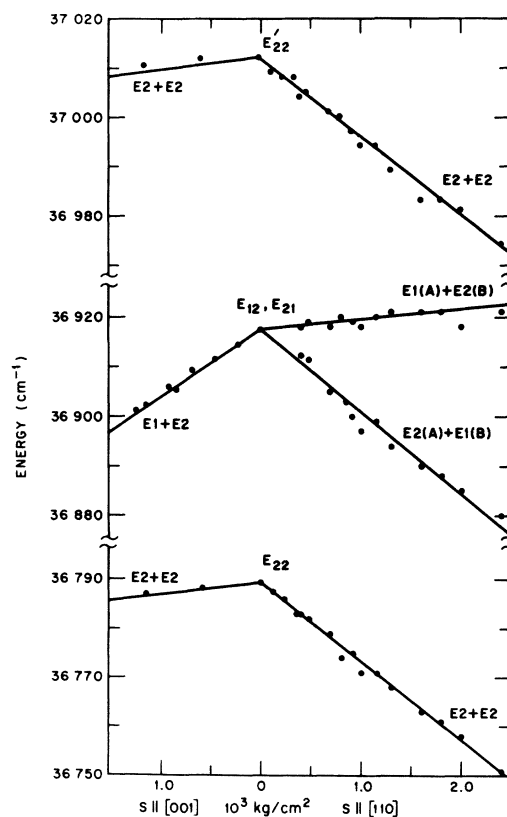


FIG. 3. Stress behavior of the double-exciton lines at 2 K. The points are those obtained experimentally; the solid lines indicate the behavior expected if the exciton-exciton interaction is independent of stress. The labels  $A$  and  $B$  refer to the two different sublattices.

seems reasonable since the magnon affects the exciton through the exchange field, which is a small perturbation; whereas, the presence of an additional exciton has an effect on the ligand field, which is more important in determining the energy states.

It is interesting that no  $E1 + E1$  ( $E_{11}$ ) transition is observed. However, it can be shown that for this transition the exchange interaction is small, and as a result, so is the transition probability. This observation and other properties of the double excitons are considered in Sec. IV.

#### IV. DISCUSSION AND THEORY

First we consider the selection rules which group theory impose on the double-exciton transitions. Loudon<sup>16</sup> discussed how exciton states are formed from the single-ion transitions and calculated the selection rules for magnon-magnon and exciton-magnon transitions, using the character tables of Dimmock and Wheeler.<sup>17</sup> The observed  $E1$  and  $E2$  transform as the  $\vec{k}=0$ ,  $\Gamma_2^+$  representation of space group  $P_{nm}$  ( $D_{2h}^{12}$ ).

The double-exciton states which are seen in absorption are combinations of single excitons at  $\vec{k}$  and  $-\vec{k}$  such that the double-exciton state transforms as a  $\vec{k}=0$  representation. The electric-dipole selection rules for double excitons formed from the single excitons at various points in the Brillouin zone are obtained simply from the tables of Dimmock and Wheeler. Only three critical points can contribute:  $X$  contributes for  $\sigma$  and  $\alpha$  polarization;  $Z$  and  $A$  contribute to  $\pi$  polarization. If the two excitons are identical, the symmetrized product of the two excitons must be used and electric-dipole transitions at  $Z$  are then forbidden. Thus, on the basis of these selection rules, we might expect that the double-exciton transitions will occur in both  $\sigma$  and  $\pi$  polarizations. Since the space-group selection rules do not indicate the observed strong polarization of the lines, we shall look more carefully at the details of the transition to see if other selection mechanisms are involved.

The observed polarizations and intensities can be explained by making the reasonable assumption that the exciton-exciton absorption intensity is primarily due to pair effects. Our program for determining the selection rules for the pair is first, determine how  $E1$  and  $E2$  transform in the site group  $D_{2h}$ ; second, using the symmetry of the pair, show that  $E_{11}$  and  $E_{22}$  can appear only in  $\sigma$ , but that ( $E_{12}, E_{21}$ ) can appear in both  $\sigma$  and  $\pi$ ; and third, show that the transition probability for  $E_{11}$  is small due to a small exchange interaction between the  $E1$  excitons.

In this discussion we shall be using the single-ion states rather than the exciton states. This is allowable since the exciton dispersion is very small.

The unitary point symmetry of the  $\text{Mn}^{2+}$  site is  $D_{2h}$  above the  $\text{MnF}_2$  Néel temperature and  $C_{2h}$  below it. In the antiferromagnetic state the site group contains the operators

$$E, C_{2x}, C_{2y}\theta, C_{2x}\theta,$$

$$I, \sigma_{xy}, \sigma_{xz}\theta, \sigma_{yz}\theta,$$

where  $\theta$  is the time-reversal operator. (The coordinate system used is shown in Fig. 1.) The unitary part of these operators are those of  $D_{2h}$ . We can make the space part of the  $E1$  and  $E2$  wave functions real if the spin-orbit coupling is small, which appears to be the case for the  $^4T_1$  state. The space part will be unaffected by the time-reversal operator. Thus, we can use the representations of  $D_{2h}$  to classify our states; however, we must remember to keep track of spin flips under time reversal. The  $D_{2h}$  representations and basis functions for  $d$  orbitals are given in Table II.

Dietz *et al.*<sup>7</sup> found that their stress results could be explained simply if  $E1$  were primarily either of  $B_2$  or  $B_3$  symmetry and  $E2$  of the opposite symmetry to  $E1$ ; that is, if  $E1$  is  $B_3$ , then  $E2$  is  $B_2$ . However, they did not definitely assign  $E1$  to a particular representation. With the aid of one assumption, which can be justified, and the stress results of Dietz *et al.*,  $E1$  can be assigned to  $B_3$  symmetry. This is discussed in Appendix A.

A pair of second-nearest-neighbor Mn ions transforms identically only under the operations  $E$  and  $\sigma_d\theta$ , where  $\theta$  is the time-reversal operator and  $\sigma_d$  is a reflection in the plane containing the pair and the  $z$  axis. The ground state, of course, is even under  $\sigma_d\theta$ . The pair excited states

$$E_{22}[^4B_{2A}(m_s = \frac{3}{2}) + ^4B_{2B}(m_s = -\frac{3}{2})]$$

and

$$E_{11}[^4B_{3A}(m_s = \frac{3}{2}) + ^4B_{3B}(m_s = -\frac{3}{2})]$$

are odd; whereas,  $E_{12}[^4B_{3A} + ^4B_{2B}]$  and  $E_{21}[^4B_{2A} + ^4B_{3B}]$  are even under the  $\sigma_d\theta$  operation. The electric-dipole transition operator (a vector) transforms as even for the two components in the mirror plane ( $z$  and  $x$  or  $y$ ) and odd for the one perpendicular to the plane ( $y$  or  $x$ ). Thus, the  $E_{11}$  and  $E_{22}$

TABLE II.  $D_{2h}$  representations and basis functions for  $d$  orbitals.

$t_2$ :	$a_1 \propto \frac{1}{2} \sqrt{3} (z^2 - y^2)$
	$b_1 \propto \sqrt{3} \ xy$
	$b_2 \propto \sqrt{3} \ xz$
$e$ :	$a'_1 \propto \frac{1}{2} (2x^2 - y^2 - z^2)$
	$b'_3 \propto \sqrt{3} \ yz$

transitions can only appear in a  $\sigma$  polarization, whereas  $E_{12}$  can appear either in  $\sigma$  or  $\pi$ . This agrees with our observation and tends to strengthen our identification of the  $E_{22}$  state.

In order to explain the absence of the  $E_{11}$  line in our spectrum, we must consider the transition probability for the double-exciton process. We assume that exchange is the important interaction giving rise to the double-exciton transition. The subsequent discussion follows closely the work of Gondaira and Tanabe,<sup>18</sup> who derived a spin-dependent transition moment for the two-magnon and exciton-magnon transitions. With slight modifications, this applies also for the exciton-exciton transition moment. The detailed expressions for the transition moment are presented in Appendix A. For our purposes here, we need only to remark that the transition probability depends on the magnitude of the exchange between two electrons, one on each ion of the Mn pair. Thus, the exchange must proceed via the intervening fluorine ions. Subsequently, the magnitude of the exchange terms depend very sensitively on the amount of mixing between the  $\text{Mn}^{2+}$   $d$  functions, given in Table II, and the surrounding  $\text{F}^-$   $p$  functions. This mixing will be small if the overlap is small or zero. If we determine from symmetry which  $d$  functions can overlap with which  $p$  functions, we find the results listed in Table III, where  $\sigma$  and  $\pi$  refer to the bond type. Of primary interest is that the  $a_1$  and  $b'_3$  orbitals have no overlap with the type-II fluorine because of symmetry. They also lie in the plane perpendicular to the type-II bond axis. Thus, we can expect little mixing between the  $a_1$ ,  $b'_3$  orbitals and the type-II fluorines.

In terms of the single-electron  $d$  orbitals, the ground state  $|^6A_1, \frac{5}{2}\rangle$  and excited states  $|^4B_3, \frac{3}{2}\rangle$  and  $|^4B_2, \frac{3}{2}\rangle$  can be written as

$$|^6A_1, \frac{5}{2}\rangle = |a_1 b_1 b_2 a'_1 b'_3\rangle,$$

TABLE III. Possible covalent mixing between Mn  $d$  orbitals and F  $p$  orbitals in  $\text{MnF}_2$ . The table indicates which of the overlap integrals,  $S = \langle d | p \rangle$  and  $\langle d | \mathcal{H} | p \rangle$  are allowed to be nonzero using the symmetry properties of the Mn-F bond. Both  $S$  and  $\langle d | \mathcal{H} | p \rangle$  have the same symmetry. The  $\sigma$  and  $\pi$  refer to the bond type.

$d$ functions	Fluorine type	
	I	II
$a_1$	$p_y (\sigma\pi), p_z (\sigma\pi)$	0
$b_1$	$p_x (\pi)$	$p_y (\pi)$
$b_2$	$p_x (\pi)$	$p_z (\pi)$
$a'_1$	$p_y (\sigma\pi), p_z (\sigma\pi)$	$p_x (\sigma)$
$b'_3$	$p_y (\sigma\pi), p_z (\sigma\pi)$	0

$$|^4B_3, \frac{3}{2}\rangle = |a_1 \bar{a}_1 b_1 b_2 a'_1\rangle, \quad (1)$$

$$|^4B_2, \frac{3}{2}\rangle = -\frac{1}{2}|a_1 b_1 \bar{b}_1 b_2 a'_1\rangle + \frac{1}{2}\sqrt{3}|a_1 b_1 b_2 \bar{b}_2 b'_3\rangle,$$

where  $\bar{a}_1$  represents a spin-down electron in orbital  $a_1$ . It can be seen that the only orbitals which are involved in a  $^6A_1 \rightarrow ^4B_3$  transition are the  $a_1$  and  $b'_3$ , which do not mix with the type-II fluorine  $p$  states. Therefore, the transfer integrals and exchange terms for a  $^6A_1 + ^6A_1 \rightarrow ^4B_3 + ^4B_3$  (or  $E_{11}$ ) transition are small because the intervening fluorine for a Mn pair is a type I for one Mn ion and a type II for the other. Thus, the transition probability is small for  $E_{11}$ . Based on this conclusion, the fact that we do not see  $E_{11}$  is also a confirmation of the assignment of  $E_1$  to  $B_3$  symmetry. For the  $E_{22}$ ,  $E_{12}$ , and  $E_{21}$  transitions, the orbitals involved can mix with both type I and type II fluorines; and thus, these have a much larger probability than  $E_{11}$ .

## V. SUMMARY

In this paper we described the observation of sharp-line transitions to the lowest-energy ( $^4T_1 + ^4T_1$ ) double-exciton states in  $\text{MnF}_2$ . We have observed three of the four possible double-exciton states containing the single excitons  $E_1$  and  $E_2$ . The identification was accomplished with the help of uniaxial stress measurements. It was found that the double-exciton energies shift under stress in the same manner as the sum of the linear energy shifts of the constituent single excitons. The absence in our absorption spectra of the particular transition  $E_1 + E_1$  was explained by using a modification of the spin-dependent transition moment of Gondaira and Tanabe. It was shown that the transition probability for  $E_1 + E_1$  is small because the exchange interaction between the electrons involved in the transition is weak. We also found that the double-exciton lines are strongly polarized, which is not indicated by the space-group selection rules. Using the second-nearest-neighbor Mn pair symmetry, however, it was demonstrated that the  $E_2 + E_2$  can only appear in  $\sigma$  and  $\alpha$  polarization, which agrees with the measured polarization. The energies of the double excitons indicate an exciton-exciton interaction energy of about  $70 \text{ cm}^{-1}$  which is negative for  $E_2 + E_2$  and positive for  $E_1 + E_2$ .

## ACKNOWLEDGMENTS

We gratefully acknowledge R. E. Dietz for helpful discussions and particularly for originally pointing out to us that the broad-band double-exciton transitions had been observed in  $\text{MnF}_2$ . We thank A. J. Williams and W. G. Emslie for technical assistance.

## APPENDIX A

In order to determine whether the  $E_1$  exciton

transforms as  $B_3$  or  $B_2$ , one reasonable assumption has to be made. It is that the sublattice which has the anticrossing of  $E1$  and  $E2$  is the one that has its type-II fluorine bond along the  $[110]$  stress direction, which is generally labeled the  $A$  sublattice. Meltzer and Lohr<sup>8</sup> made this assumption, which they supported by comparing their crystalline field calculations on the stress dependence of the energy splitting between  $B_3$  and  $B_2$  with the experimental values. They found that the stress behavior of the  $E1-E2$  splitting could be simply related to changes in the difference between the type-I and type-II Mn-F bond lengths. A  $[110]$  stress changes the relative bond lengths on the  $A$  sublattice, whereas its effect on sublattice  $B$  is a change in the angle between Mn-F bonds, but little change in the relative bond lengths. Therefore, it is the  $A$  sublattice which is affected more by a  $[110]$  stress.

With this information, we can use the stress results of Dietz *et al.*<sup>7</sup> to find the symmetry of  $E1$ . The reasoning proceeds as follows: First, it is observed that only one state,  $B_3$  or  $B_2$ , couples to the magnons in  $\sigma$  polarization. For  $[110]$  stress,  $\sigma 1A$  (the magnon sideband of  $E1$ ) loses intensity as the stress is increased. Second, if we look at sublattice  $B$ , the more intense sideband  $\sigma 2B$  appears only with its electric-dipole vector parallel to the  $x$  axis of sublattice  $B$ . Third, Tanabe and Gondaira<sup>13</sup> from exciton-magnon pair symmetries showed that the  $B_2$  magnon sideband had a transition moment only along the  $x$  axis and  $B_3$  only along the  $y$  axis. Therefore,  $B_2$  must be associated with  $\sigma 2B$  and  $E2$ , and  $B_3$  with  $E1$ .

The conclusion that  $E1$  must be of  $B_3$  symmetry was also reached by Meltzer and Lohr. They did not use the above argument, but used a Hückel calculation on the  $\text{MnF}_6^{4-}$  complex and showed that  $B_3$  must lie lowest in energy if an anticrossing were to take place.

#### APPENDIX B

Following Gondaira and Tanabe,<sup>19</sup> the spin-dependent transition moment for a pair of ions labeled

$a$  and  $b$  can be written

$$\begin{aligned} \tilde{\Pi}(aa^*bb^*) = & \sum_{ii'} \sum_{jj'} \tilde{\pi}(ai' - i, bj' - j) \\ & \times [\tilde{\mathbf{S}}_a(i' - i) \cdot \tilde{\mathbf{S}}_b(j' - j)], \end{aligned} \quad (\text{B1})$$

where

$$\tilde{\mathbf{S}}_a(i' - i) = \sum_{mm'} c_{ai'm'}^\dagger c_{aim} \langle m' | \tilde{\mathbf{S}} | m \rangle.$$

The  $i$  and  $j$  refer to one-electron orbitals centered on Mn ions  $a$  and  $b$ , respectively. The  $c_{ai'm'}^\dagger$  operators create an electron on ion  $a$  in orbital  $i'$  with spin projection  $m'$ . The transition moment  $\tilde{\pi}(ai' - i, bj' - j)$  contains exchange terms such as the following:

$$\begin{aligned} \tilde{\pi}(ai' - i, bj' - j) = & \frac{h(bj' - ai)}{U} \langle ai' | \tilde{\mathbf{p}} | bj \rangle \\ & + \sum_{\mu k} \frac{\langle bj' ai' | \mathcal{K} | bj \mu k \rangle \langle \mu k | \tilde{\mathbf{p}} | ai \rangle}{E(bj', ai) - E(bj, \mu k)} \\ & + \frac{\langle ai' | \tilde{\mathbf{p}} | \mu k \rangle \langle bj' \mu k | \mathcal{K} | bj ai \rangle}{E(bj', \mu k) - E(bj, ai)} \\ & + \text{terms with } a \text{ and } b \text{ interchanged.} \end{aligned} \quad (\text{B2})$$

In this expression,  $h(bj' - ai)$  is a transfer integral,  $U$  is the average electrostatic repulsion of two electrons on the same ion,  $\mu k$  can be any empty or singly occupied state of ion  $a$  or  $b$ ,  $\mathcal{K}$  is the Hamiltonian,

$$\begin{aligned} \langle bj' ai' | \mathcal{K} | bj \mu k \rangle = & \int d\tau (1) d\tau (2) \\ & \times \phi_{bj'}(1) \phi_{ai'}(2) H \phi_{bj}(2) \phi_{\mu k}(1), \end{aligned}$$

and  $\tilde{\mathbf{p}}$  is the dipole operator. The first term in expression (2) arises from direct mixing of the wave functions of ions  $a$  and  $b$ . The coefficient  $h(bj' - ai)/U$  expresses the amount of orbital  $ai$  mixed into orbital  $bj'$ . In the theory of exchange interactions these transfer integrals give rise to Anderson's kinetic exchange.<sup>19</sup> The second term in (2) originates from direct or potential exchange on either ion.

<sup>1</sup>J. Woods Halley and I. Silvera, Phys. Rev. Letters **15**, 654 (1965); Phys. Rev. **149**, 415 (1966); **149**, 423 (1966).

<sup>2</sup>S. J. Allen, Jr., R. Loudon, and P. L. Richards, Phys. Rev. Letters **16**, 463 (1966).

<sup>3</sup>R. L. Greene, D. D. Sell, W. M. Yen, A. L. Schawlow, and R. M. White, Phys. Rev. Letters **15**, 656 (1965).

<sup>4</sup>D. D. Sell, R. L. Greene, and Robert M. White, Phys. Rev. **158**, 489 (1967).

<sup>5</sup>J. Ferguson, Australian J. Chem. **21**, 307 (1968).

<sup>6</sup>J. P. Van der Ziel and H. J. Guggenheim, Phys. Rev. **166**, 479 (1968).

<sup>7</sup>R. E. Dietz, A. Missetich, and H. J. Guggenheim, Phys. Rev. Letters **16**, 841 (1966).

<sup>8</sup>R. S. Meltzer and L. L. Lohr, J. Chem. Phys. **49**, 541 (1968).

<sup>9</sup>S. Washimiya and K. Gondaira, J. Phys. Soc. Japan **23**, 1 (1967).

<sup>10</sup>R. E. Dietz and A. Missetich, in *Proceedings of the Conference on Localized Excitations in Solids, Irvine, California*, 1967 (Plenum, New York, 1968), p. 366.

<sup>11</sup>R. E. Dietz, A. E. Meixner, H. J. Guggenheim, and A. Missetich, Phys. Rev. Letters **21**, 1067 (1968).

<sup>12</sup>M. Tinkham, *Group Theory and Quantum Mechanics* (McGraw-Hill, New York, 1964), p. 327.

<sup>13</sup>Y. Tanabe and K. Gondaira, J. Phys. Soc. Japan **22**, 573 (1967).

<sup>14</sup>D. D. Sell, Appl. Opt. **9**, 1926 (1970).

<sup>15</sup>D. D. Sell and E. O. Kane, Phys. Rev. **185**, 1103 (1969).

<sup>16</sup>R. Loudon, Advan. Phys. **17**, 243 (1968).

<sup>17</sup>J. O. Dimmock and R. G. Wheeler, Phys. Rev. **127**, 391 (1962).

<sup>18</sup>K. Gondaira and Y. Tanabe, J. Phys. Soc. Japan **21**, 1527 (1966).

<sup>19</sup>P. W. Anderson, in *Solid State Physics* (Academic, New York, 1963), Vol. 14, p. 99.

## Kondo Effect in Amorphous Fe-Pd-Si and Co-Pd-Si Alloys\*

Ryusuke Hasegawa and C. C. Tsuei

*W. M. Keck Laboratory of Engineering Materials, California Institute of Technology, Pasadena, California 91109*

(Received 17 August 1970)

A Kondo-type resistivity minimum has been found in amorphous alloys obtained by rapid quenching from the liquid state and having the compositions  $\text{Fe}_x\text{Pd}_{80-x}\text{Si}_{20}$  and  $\text{Co}_x\text{Pd}_{80-x}\text{Si}_{20}$ , in which  $x$  (in at. %) varies from 0 to 7 for Fe and from 0 to 11 for Co. Magnetic measurements indicate that these alloys become ferromagnetic at low temperatures. The resistivity and magnetoresistivity data are analyzed by the existing theories on the  $s$ - $d$  exchange interaction. The results demonstrate that the coexistence of the resistivity minimum and ferromagnetism can be explained by the presence of small amounts of paramagnetic ions free from mutual interactions. This result is confirmed by magnetoresistivity measurements. The estimated values for the  $s$ - $d$  exchange integral are  $-0.62$  eV for the Fe-Pd-Si alloys and  $-0.42$  eV for the Co-Pd-Si alloys.

### I. INTRODUCTION

As shown by Kondo,<sup>1</sup> the dynamical nature of the localized spin system leads to the resistivity-minimum phenomenon in magnetically dilute alloys. This has been confirmed by a number of experimental results demonstrating that the Kondo logarithmic term in the resistivity is associated with the paramagnetic nature of the alloys. The existence of the noninteracting localized spin system has been assumed in later theoretical<sup>2</sup> and experimental<sup>3</sup> papers. Attempts to take into account the interacting localized spins in terms of an internal field have been made by several workers.<sup>4-8</sup> They found that the Kondo logarithmic term is suppressed by the internal field. Experimentally this has been evidenced by the decrease<sup>7,8</sup> of the absolute slope of the  $\ln T$  term in the resistivity with increasing magnetic solute concentration and/or by the appearance of the resistivity maximum<sup>9</sup> below the resistivity minimum temperature. The latter phenomenon seems to be associated with the onset of magnetic ordering. Recent work<sup>10</sup> on both ferromagnetic and paramagnetic Ni-Cu alloys demonstrates that the Kondo effect disappears in the ferromagnetic alloys. These observations seem to indicate that the Kondo effect does not coexist with ferromagnetism in crystalline alloys which have been studied extensively so far.

In this paper, we discuss the results obtained for noncrystalline Pd-Si alloys containing Fe or Co and show that these results imply the coexistence of the Kondo effect with ferromagnetism in the amorphous

alloys. The experimental technique for the present measurements is similar to that presented in previous papers.<sup>11,12</sup> The existence of a resistivity minimum in a ferromagnetic amorphous  $\text{Fe}_{80}\text{P}_{13}\text{C}_7$  alloy has been reported already.<sup>13</sup> This, however, is not subject to a wide change in the magnetic-metal concentration. The present Pd-Si base amorphous alloys can contain from 0- to 7-at. % Fe or from 0- to 11-at. % Co, serving as one of the most suitable systems to study systematically the cases of dilute (paramagnetic) and concentrated (ferromagnetic) alloys.

### II. RESULTS AND DISCUSSIONS

#### A. Amorphous $\text{Fe}_x\text{Pd}_{80-x}\text{Si}_{20}$ Alloys

It has been established that the amorphous  $\text{Fe}_x\text{Pd}_{80-x}\text{Si}_{20}$  alloy ( $0 < x \leq 7$ ) behaves like a paramagnet at high temperatures and like a ferromagnet at low temperatures.<sup>14</sup> The results of these measurements are summarized in Table I. Above

TABLE I. Results of the magnetic measurements for the  $\text{Fe}_x\text{Pd}_{80-x}\text{Si}_{20}$  alloys (taken from Ref. 14).

$x$	$\mu_{\text{eff}} (\mu_B/\text{atom})$ $T_d < T < 300^\circ\text{K}$	$T_d$ ( $^\circ\text{K}$ )	$\theta_p$ ( $^\circ\text{K}$ )	$T_c$ ( $^\circ\text{K}$ )
0.5	5.73	1.7	1	...
1	5.78	45	11	...
3	5.85	50	30	...
5	5.60	95	64	...
7	5.60	160	110	28